RSC Applied Polymers

ROYAL SOCIETY OF CHEMISTRY

PAPER

View Article Online
View Journal | View Issue

Check for updates

Cite this: *RSC Appl. Polym.*, 2024, **2**, 838

Salicylhydroxamic acid containing structural adhesive†

Md Saleh Akram Bhuiyan, Kan Wang, Fatemeh Razaviamri and Bruce P. Lee *

Received 22nd April 2024,
Accepted 8th June 2024

DOI: 10.1039/d4lp00139g

rsc.li/rscapplpolym

The feasibility of utilizing salicylhydroxamic acid (SHAM) as a new adhesive molecule for designing structural adhesives is investigated in this study. SHAM-containing polymers were prepared with a hydroxyethyl methacrylate (HEMA) or methoxyethyl acrylate (MEA) backbone and mixed with polyvinylidene fluoride (PVDF). PVDF was included to increase the cohesive property of the adhesive through hydrogen bond (H-bond) formation with the adhesive polymers. SHAM-containing adhesive demonstrated lap shear adhesion strength (S_{adh}) greater than 0.9 MPa to glass, metal, and polymeric surfaces. Adhesive formulations with elevated SHAM-content also demonstrated increased adhesive properties with S_{adh} values reaching as high as 4.8 MPa. Due to the physically crosslinked nature of these adhesives, formulations with extensive H-bonding resulted in strong adhesion and stability. HEMA consists of a terminal hydroxyl group with both H-bond donor and acceptor, which enabled HEMA-containing adhesives to demonstrate strong adhesion even without PVDF. On the other hand, MEA contains a methoxy group that lacks H-bond donors for forming H-bonding and MEA-containing adhesives required PVDF to provide H-bond acceptors to increase its cohesive property. An aging study was performed on the bonded joints. While the adhesive joints did not demonstrate any reduction in S_{adh} values over 25 days when incubated in a dry condition, S_{adh} values decreased by 80% over 48 h when incubated in water. This is potentially due to the hydrophilic and physically crosslinked nature of the adhesive. Nevertheless, the SHAM-containing adhesive outperformed a catechol-containing adhesive and epoxy glue and is a promising new adhesive molecule for designing structural adhesives.

Introduction

Adhesives are utilized to bond two dissimilar surfaces together. They are commonly used in many applications ranging from sticky tapes,[1] tissue adhesives,[2] and dental adhesives[3] to consumer packaging[4] and the automobile industry.[5] In designing better performing adhesives, scientists have incorporated biomimetic chemistries in their designs.[6–8] One of the most frequently studied bioinspired adhesive systems is inspired by mussel adhesive proteins.[9–11] One of the key constituents in these adhesive proteins is the amino acid L-3,4-dihydroxyphenyl alanine (DOPA), which is responsible for strong interfacial bonding.[12,13] DOPA contains a catechol side chain (Fig. 1), which can participate in a diverse range of interfacial interactions such as hydrogen bonding (H-bonding), π–π interaction, cation–π interaction, and metal ion coordination.[7,10,14] This enables catechol-containing adhesives to adhere to a diverse range of surfaces.[15] However, catechol is prone to oxidation in an aqueous and basic environment, which results in poor adhesive properties.[16–18] Preserving the reduced and adhesive form of catechol is one of the major challenges associated with using this biomimetic strategy in designing adhesives.

Salicylhydroxamic acid (SHAM) is a compound that has been utilized in anti-aging cosmetic products,[19] antitubercular therapeutic applications,[20,21] and multi-targeted drug therapy.[22] It was also used in textile dye modification,[23] molecular detection,[24] wastewater purification,[25] and metal ion chelation.[26,27] SHAM contains a benzyl hydroxamic acid and

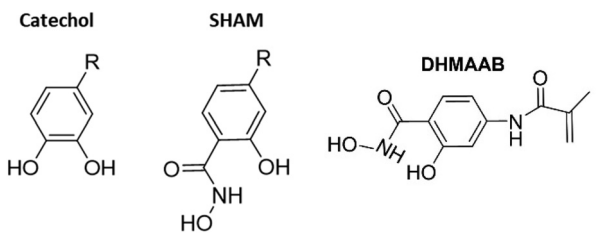

Fig. 1 Chemical structures of catechol, SHAM and SHAM-containing monomer, *N*,2-dihydroxy-4-methacrylamidobenzamide (DHMAAB).

Department of Biomedical Engineering, Michigan Technological University, 1400 Townsend Drive, Houghton, Michigan 49931, USA. E-mail: bplee@mtu.edu

† Electronic supplementary information (ESI) available. See DOI: https://doi.org/10.1039/d4lp00139g

hydroxyl group and resembles the chemical structure of catechol (Fig. 1). Recently, our lab demonstrated the ability for SHAM to bind to various surfaces (glass, titanium, polystyrene, and amine-functionalized surface) with interfacial bonding properties that were comparable to those of catechol.[28] Unlike catechol that undergoes irreversible oxidation, SHAM is highly resistant to base treatment and can fully recover its adhesive properties even after its exposure to pH as high as 11. This indicates that SHAM can be utilized to design an adhesive with improved chemical stability when compared to catechol.

Our prior work mainly focused on characterizing the interfacial bonding behavior of SHAM.[28] However, the ability for SHAM to function as an adhesive moiety in a structural adhesive has never been demonstrated. This study aims to determine the feasibility for SHAM to function as an adhesive molecule in a structural adhesive with enhanced performance. To create a structural adhesive with elevated adhesive properties, an adhesive needs to have a balance of elevated interfacial bonding and cohesive properties.[29,30] To improve the cohesive property of SHAM-containing adhesives, these polymers were blended with polyvinylidene fluoride (PVDF). PVDF has been widely utilized as a binder to create physical crosslinking within a polymer system and to provide structural support.[31] The vinylidene fluoride units of PVDF can participate in H-bonding with electronegative donors such as oxygen atoms.[32] Incorporation of PVDF has been previously utilized in the preparation of coatings,[33] battery design,[34] sensors,[35] and wearable electronics.[36]

In this report, various SHAM-containing adhesive copolymers were prepared by polymerizing *N*,2-dihydroxy-4-methacrylamidobenzamide (DHMAAB) (Fig. 1), a SHAM-containing monomer, with hydroxyethyl methacrylate (HEMA) or methoxyethyl acrylate (MEA). These copolymers were then mixed with PVDF to create a physically crosslinked adhesive. The effect of adhesive composition (*e.g.*, PVDF content, SHAM content, polymer backbone, *etc.*) on lap shear adhesion strength was evaluated (Fig. S1†). Additionally, the adhesive properties of SHAM-containing adhesives were compared with those of catechol and epoxy-based adhesives. Finally, the effect of aging under both dry and wet conditions on adhesion was investigated.

Materials and methods

Materials

HEMA, MEA, 1-methyl-2-pyrrolidinone (NMP; ≥99.0%, ACS reagent), polyvinylidene fluoride (PVDF; average $M_w \sim 180\,000$ Da and average $M_n \sim 71\,000$ Da), silicon oil, and dimethyl sulfoxide-d6 (DMSO-d6) were purchased from Sigma-Aldrich (St Louis, MO). Dimethylformamide (DMF; 99.8%, anhydrous), diethyl ether (anhydrous, ACS grade), quartz glass (glass slide), acetone (≥99.5%), isopropanol (IPA; ACS grade), and ethanol (200 proof, anhydrous) were purchased from Fisher Scientific (Fair Lawn, NJ). 2,2′-Azobis(isobutyronitrile) (AIBN) was purchased from Wako Pure Chemical Industries, Ltd (Osaka, Japan). High-strength grade 5 titanium (Ti surface (Ti6Al4V), 0.016″ thick) sheet, multipurpose 6061 aluminum sheets (0.016″ thick), clear scratch- and UV-resistant cast poly(methyl methacrylate) (PMMA) sheet (1/16″ thick), optically clear epoxy structural adhesive (Double/Bubble® Epoxy Extra Fast Setting, H.B. Fuller Company Vadnais Heights, MN), and 100 g test weight were purchased from McMaster-Carr (Elmhurst, IL). Two adhesive monomers, dopamine methacrylamide (DMA) and DHMAAB, were prepared according to previously published protocols.[18,28]

Preparation of adhesive copolymers

Adhesive copolymers prepared in this work are shown in Fig. 2. The copolymers were prepared by combining up to 50 mol% of the adhesive monomer (DHMAAB or DMA) with HEMA or MEA as the backbone through thermo-initiated free radical polymerization (Table 1). In the abbreviations of these copolymers, the subscripted numerical value that appears

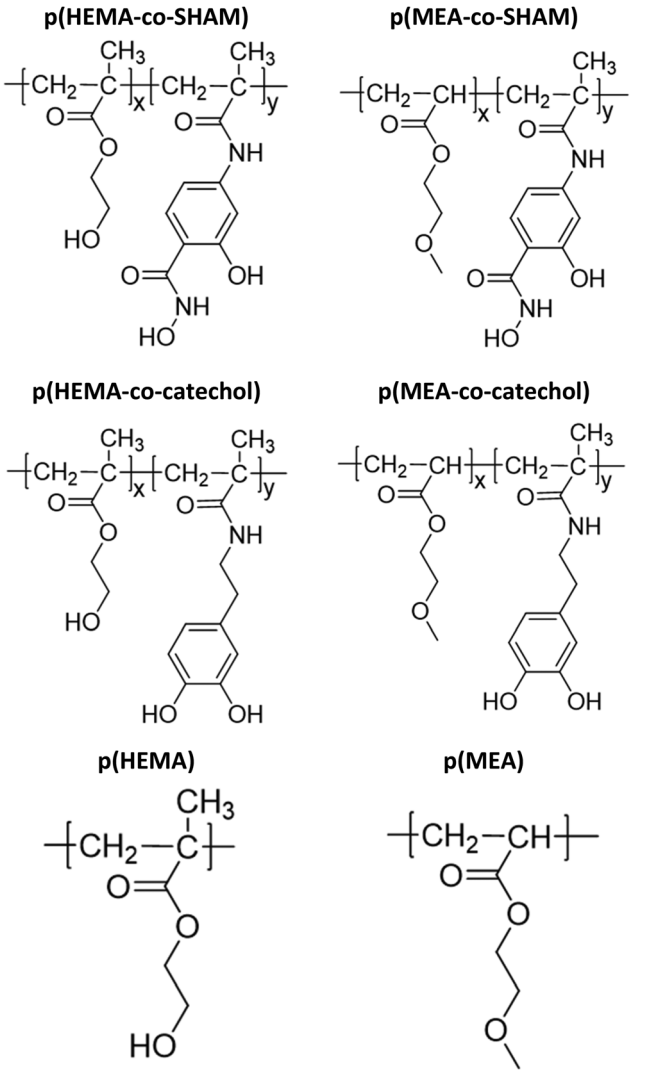

Fig. 2 Chemical structures of various adhesive copolymers prepared in this work.

Table 1 Feed and actual mol% of monomers in the adhesive polymers

	Mol% in feed		Actual mol% in polymer based on ^{1}H NMR	
Abbreviation	DMHBAA	DMA	DMHBAA	DMA
p(HEMA)	0	0	0	0
p(HEMA-*co*-SHAM$_{10}$)	10	0	6.8	0
p(HEMA-*co*-SHAM$_{50}$)	50	0	33.7	0
p(MEA)	0	0	0	0
p(MEA-*co*-SHAM$_{10}$)	10	0	10.8	0
p(MEA-*co*-SHAM$_{50}$)	50	0	43.2	0
p(HEMA-*co*-catechol$_{10}$)	0	10	0	8.0
p(MEA-*co*-catechol$_{10}$)	0	10	0	9.9

after SHAM or DMA represents the mol% of SHAM or DMA used during the reaction. For example, p(HEMA-*co*-SHAM$_{10}$) was prepared using 10 mol% DHMAAB relative to HEMA during the synthesis of the polymers, while p(HEMA-*co*-catechol$_{10}$) was prepared using 10 mol% DMA. Using p(HEMA-*co*-SHAM$_{10}$) as an example, 1 mmol of HEMA, 0.1 mmol of DHMAAB, and 0.03 mmol of AIBN were dissolved in 1 mL of DMF. The reaction mixtures were stirred at 500 rpm and heated in a 70 °C silicone oil bath overnight under nitrogen. After cooling to room temperature, the polymer was precipitated in 40 mL of diethyl ether. The precipitated polymer was collected through centrifugation at 5000 rpm for 5 minutes and vacuum-dried for 24 hours before use. DMA-containing polymers were prepared in the same manner by replacing DHMAAB with DMA. Control polymers, p(HEMA) and p(MEA), were prepared without DHMAAB or DMA.

The chemical compositions of all the prepared copolymers were investigated by proton nuclear magnetic resonance (^{1}H NMR, Ascend 500 MHz, Bruker, MA) spectroscopy using DMSO-d6. A gel permeation chromatography (GPC, Shimadzu HPLC Nexera Series) system equipped with a UV detector (SPD-40, Shimadzu), a refractive index detector (RID-20A, Shimadzu), and a multiple-angle light scattering detector (miniDAWN, Wyatt) was used to determine the number average molecular weight (M_n), the weight average molecular weight (M_w), and the polydispersity index (PDI) of the polymers. 20 μL of polymer solution (5 mg mL^{-1} in DMSO) was injected and eluted at 0.5 mL min^{-1} through a Shodex OHpak LB-803 column using DMF (HPLC grade) as the mobile phase while keeping the column in an oven at a temperature of 40 °C.

Preparation of the surface substrates

The dimensions of all the surface substrates used in this work were 1 inch × 0.5 inch. Both the glass and PMMA substrates used in this work underwent a 2-step cleaning process. In the first step, the substrate was cleaned with IPA, acetone, and ethanol for 5 minutes in the sonication bath. Subsequently, the substrate surface was treated with oxygen plasma (200 W and 200 mTorr; Trion Technology Phantom II, Clearwater, FL) for 5 minutes. The metal surfaces underwent a 3-step cleaning process. Initially, the metal substrate surfaces were polished with a sandpaper. Then the substrates were cleaned with IPA, acetone, and ethanol for 5 minutes in a sonication bath. Finally, all these substrates were treated with oxygen plasma for 5 minutes. These substrates were stored in a vacuum sealed container before use.

Preparation of the adhesive precursor

The adhesive precursor solution was prepared by combining two polymer solutions. One of the solutions contained 10 wt% of PVDF, while the other contained the synthesized adhesive copolymer with a concentration of 150 mg mL^{-1}. The solvent used in these mixtures was prepared by mixing NMP and acetone with a weight ratio of 75 : 25. The adhesive precursor was then placed on an orbital shaker for 12 hours with gentle nutation to ensure complete polymer dissolution and the preparation of a copolymer-PVDF blend.

Lap shear adhesion test

To prepare the adhesive joint, 10 μL of adhesive precursor solution was added onto the surface of both substrates (Fig. S2 and S3†). The substrates were then kept in open air at room temperature for 15 minutes to evaporate the acetone and in an oven for 10–15 minutes at 60 °C for the partial evaporation of NMP. The adhesive-coated area of the two substrates was compressed together with binder clips to create a lap shear joint with an overlapped surface area of 64.5 mm^2. 20 μl of adhesive precursor solution was utilized to create a lap shear joint with an overlapped area of 129 mm^2. The prepared samples were kept in an oven at 60 °C overnight to evaporate all the solvents before performing the lap shear adhesion test. Lap shear adhesion test was performed by pulling the substrates at a rate of 0.022 mm s^{-1} using a universal testing machine (Acumen, MTS Systems Corporation, Eden Prairie, MN) following ASTM D1002 guidelines. The adhesion strength (S_{adh}) was calculated by dividing the maximum load by the overlapped area of the adhesive joint.[37]

Aging analysis of adhesives

Aging analysis of the adhesive was performed in air and underwater. The adhesive joints were exposed to the open air for up to 25 days (temperature ≈ 21.5 °C, humidity ≈ 20%). Attenuated total reflectance Fourier transform infrared (ATR-FTIR) spectroscopy technique (IRTracer-100, Shimadzu Corporation; Kyoto, Japan) was used to evaluate any chemical changes after 5 days while lap shear adhesion testing was performed after 25 days. To investigate the effect of underwater submersion on the adhesive joint, the specimens were immersed in 50 mL of deionized (DI) water for up to 48 hours prior to lap shear adhesion testing.

Statistical analysis

The SigmaPlot software was utilized for statistical analysis. One-way analysis of variance (ANOVA) with Tukey method and Student's *t*-test were used for comparing mean values from multiple and two groups, respectively, using a *p*-value of 0.05.

Results

A series of SHAM-containing polymers were prepared by copolymerizing DHMAAB with either HEMA or MEA (Fig. 2). The chemical composition of the prepared copolymers was verified using ^{1}H NMR (Fig. S4–S11†). Based on the NMR analysis, these polymers contained either HEMA or MEA backbone with a SHAM content of up to 43 mol% (Table 1). Incorporation of SHAM was slightly lower when it was copolymerized with HEMA (~66–68%) when compared with MEA-containing polymer (>85%). A similar result was observed for the copolymerization of DMA. GPC was utilized to determine the molecular weight of these samples (Table S1†). These polymers exhibited elevated molecular weights (10^4–10^6 Da) and relatively large polydispersity index values (>3), potentially due to the fast free-radical polymerization process.

The adhesive polymers were blended with PVDF, which serves as a binder to increase the cohesive property of these adhesive formulations. The presence of SHAM and PVDF were confirmed using ATR-FTIR analysis (Fig. S12†). The characteristic peaks of SHAM were observed at 1488 cm^{-1} and 1521 cm^{-1} (Fig. 3a, red dashed line) in the ATR-FTIR spectra, regardless of the presence of PVDF.[28] The peaks appearing around 1720–1730 cm^{-1} (Fig. S12,† red dashed line) corresponded to the vibration modes of the C=O bands in MEA and HEMA. Formulations that contained PVDF demonstrated peaks at 837 and 876 cm^{-1} which were associated with the asymmetric stretching of CF_2 and the rocking of CH_2 in PVDF[38] (Fig. 3b).

SHAM-containing adhesives exhibited elevated adhesive strength when tested using glass substrates. p(HEMA-*co*-SHAM$_{10}$) exhibited S_{adh} that averaged around 2.3 MPa while p(MEA-*co*-SHAM$_{10}$) exhibited a S_{adh} of 1.8 MPa (Fig. 4). SHAM interacts with the glass surface through H-bonding[28] and these adhesives exhibited a mixture of adhesive and cohesive failure in the detached surfaces (Fig. 4c). Additionally, SHAM-containing adhesives exhibited a significantly higher adhesive strength when compared to catechol-containing adhesives (S_{adh} = 1.7 MPa and 0.8 MPa for p(HEMA-*co*-Catechol$_{10}$) and p(MEA-*co*-Catechol$_{10}$), respectively). These findings corroborated with our previous report where SHAM exhibits higher

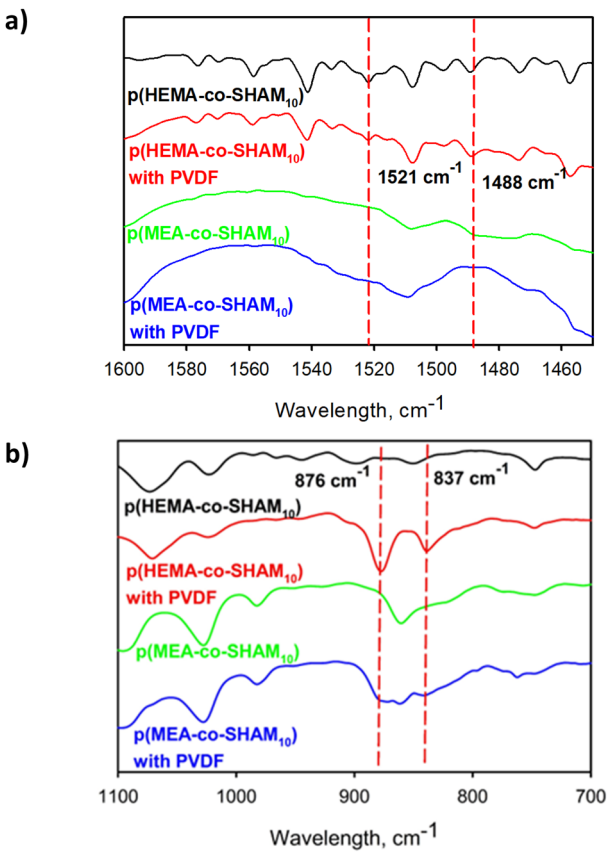

Fig. 3 ATR-FTIR spectra of p(HEMA-*co*-SHAM$_{10}$) and p(MEA-*co*-SHAM$_{10}$) with and without PVDF in the range of (a) 1600–1450 cm^{-1} and (b) 1100–700 cm^{-1}.

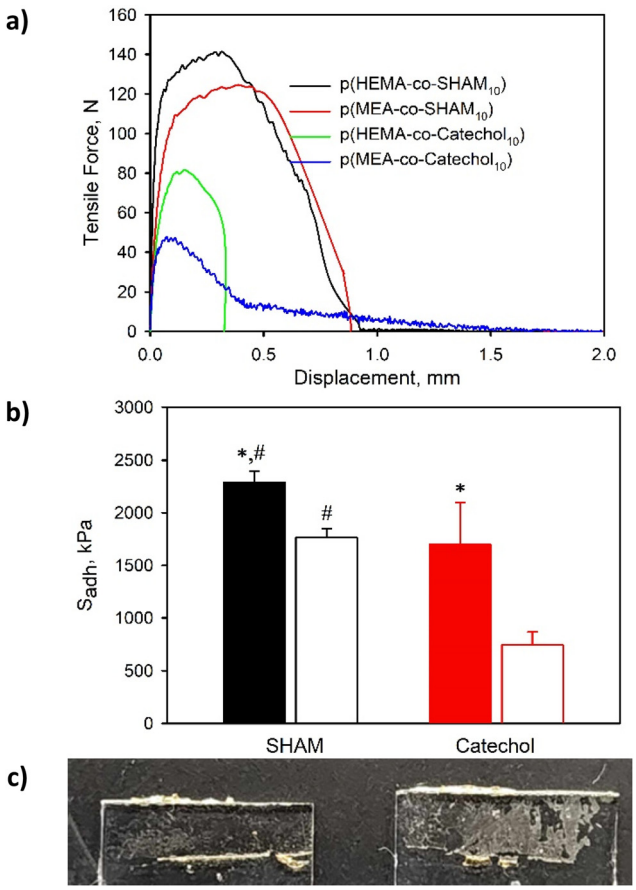

Fig. 4 (a) Lap shear curve for adhesive joints formed using various SHAM and catechol-containing polymers tested using glass substrates. (b) S_{adh} of SHAM and catechol-containing polymers polymerized with HEMA (filled bars) and MEA (empty bars) backbone. (c) Image of the sample prepared with p(HEMA-*co*-SHAM$_{10}$) after the lap shear adhesion test. The adhesives were prepared by maintaining a copolymer to PVDF weight ratio of 85 : 15, with an overlapped area of 64.5 mm^2 and a coating density of 4 mg cm^{-2}. *p < 0.05 when compared to MEA-containing adhesive. #p < 0.05 when compared to catechol-containing adhesive (n = 3).

interfacial bonding properties to glass surfaces when compared to catechol.[28] In addition, adhesives with a HEMA backbone exhibited stronger adhesive strength when compared to adhesives with a MEA backbone regardless of the adhesive molecule. The pendant hydroxyl group of the HEMA backbone likely played an important role in both interfacial bonding and cohesion as it contains both a H-bond donor and acceptor. On the other hand, MEA contains a methoxy group and lacks H-bond donors for forming strong cohesion through H-bonding.

SHAM-containing adhesives also demonstrated strong adhesion to metal and polymer surfaces regardless of the polymer backbone with S_{adh} of 0.9 MPa or higher (Fig. 5 and S13†). Similar to glass substrates, the calculated S_{adh} values were significantly higher for HEMA-containing adhesives (S_{adh} = 1.3–2.3 MPa) when compared to their MEA counterparts (S_{adh} = 0.9–1.3 MPa). Interestingly, SHAM exhibited the highest S_{adh} values when adhered to glass surfaces. Consistent with earlier observations, a mixture of adhesive and cohesive failures was observed on the separated substrates irrespective of the substrate material or the polymer backbone of the adhesive. However, it is noteworthy that the metal surface exhibited a considerably cleaner surface after detachment (Fig. S14†). This suggested that SHAM-containing adhesives are more likely to result in adhesive failure when tested using metal substrates. This is consistent with our previous finding where SHAM demonstrated higher interfacial bonding energy to glass surfaces than metal substrates.[28]

The effect of adhesive coating density and overlapped area of the adhesive joint on S_{adh} was also determined. Average S_{adh} values increased significantly when the coating density increased from 2 to 4 mg cm^{-2}, regardless of the copolymer backbone (Fig. 6 and S15†). This increase in coating density corresponded to increased SHAM concentration within the adhesive, resulting in an increase in adhesive strength.

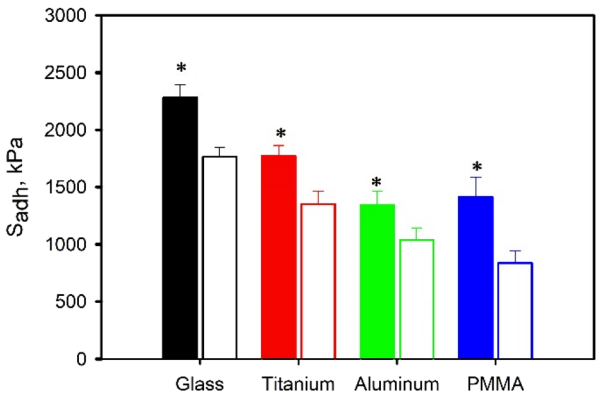

Fig. 5 S_{adh} for p(HEMA-*co*-SHAM$_{10}$) (filled bars) and p(MEA-*co*-SHAM$_{10}$) (empty bars) tested using different substrates. The adhesives were prepared by maintaining a copolymer to PVDF weight ratio of 85 : 15, with an overlapped area of 64.5 mm^2 and a coating density of 4 mg cm^{-2}. *p < 0.05 when compared to MEA-containing adhesive (n = 3).

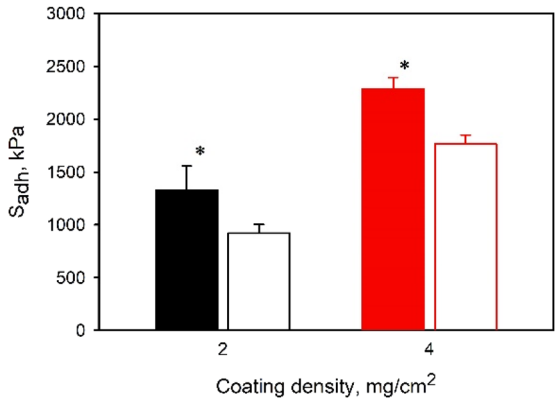

Fig. 6 S_{adh} of the adhesives prepared at different coating density in the adhesive joint using p(HEMA-*co*-SHAM$_{10}$) (filled bars) and p(MEA-*co*-SHAM$_{10}$) (empty bars). The adhesives were prepared by maintaining a copolymer to PVDF weight ratio of 85 : 15, with an overlapped area of 64.5 mm^2. *p < 0.05 when compared to MEA-containing adhesive (n = 3).

Conversely, S_{adh} was not affected by the change in the overlapped area of the adhesive joints (Fig. 7), given that S_{adh} was normalized by the area of overlap. The maximum force measured increased proportionally with increasing area of lap shear joint as expected (Fig. S16†).

Effect of the adhesive copolymer to PVDF weight ratio on S_{adh} was further examined (Fig. 8a and S17†). In general, increasing the adhesive copolymer content in the adhesive formulation increased S_{adh} as expected. PVDF lacks adhesive properties and does not contribute to interfacial bonding. For adhesive with HEMA backbone, 100 wt% p(HEMA-*co*-SHAM$_{10}$) demonstrated the strongest adhesion strength (2.8 MPa). On the other hand, 100 wt% p(MEA-*co*-SHAM$_{10}$) was poorly adhesive (0.15 MPa) and the highest S_{adh} was observed for a copolymer to PVDF weight ratio of 85 : 15 (1.8 MPa). This result highlights the contribution of the adhesive backbone on adhesion. HEMA contains a pendant hydroxyl group, which

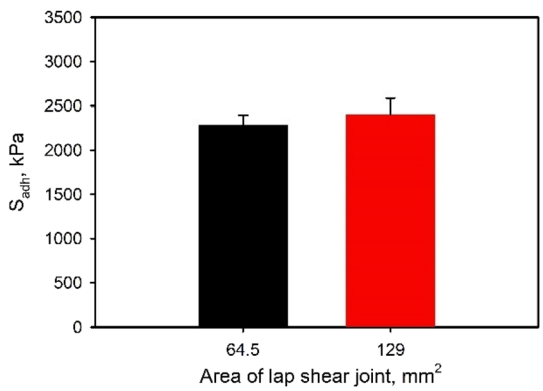

Fig. 7 S_{adh} of the adhesives prepared with p(HEMA-*co*-SHAM$_{10}$) tested with different overlapped area in the adhesive joint. The adhesives were prepared by maintaining a copolymer to PVDF weight ratio of 85 : 15 and a coating density of 4 mg cm^{-2} (n = 3).

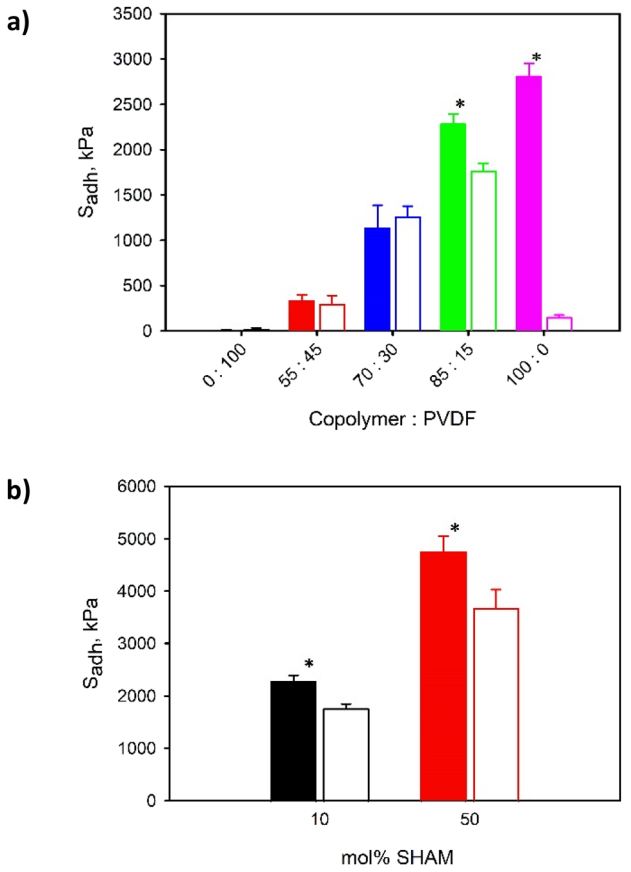

Fig. 8 (a) S_{adh} of the adhesive formulations prepared with different adhesive copolymer to PVDF weight ratio using p(HEMA-*co*-SHAM$_{10}$) (filled bars) and p(MEA-*co*-SHAM$_{10}$) (empty bars). (b) S_{adh} of the adhesive prepared with different mol% of SHAM in the reaction feed tested at a copolymer to PVDF weight ratio of 85 : 15, with an overlapped area of 64.5 mm^2 and a coating density of 4 mg cm^{-2}. *p < 0.05 when compared to MEA-containing adhesive (n = 3).

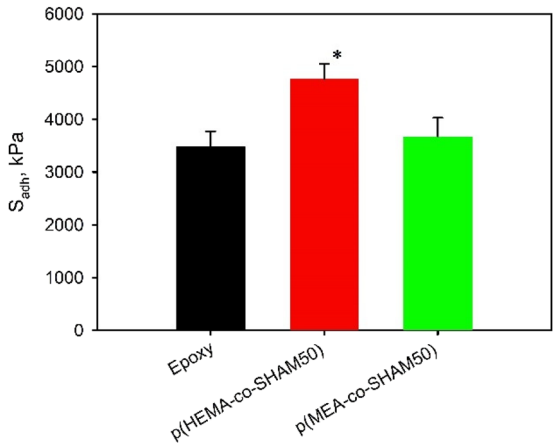

Fig. 9 S_{adh} of epoxy, p(HEMA-*co*-SHAM$_{50}$), and p(MEA-*co*-SHAM$_{50}$). Adhesive contained a copolymer to PVDF weight ratio of 85 : 15, with an overlapped area of 64.5 mm^2 and a coating density of 4 mg cm^{-2}. *p < 0.05 when compared to epoxy (n = 3).

can function both as a H-bond donor and acceptor to promote cohesive interaction needed for strong adhesion. However, MEA consists of a methoxy group and is missing H-bond donors. Adding PVDF likely increased the cohesive property of MEA-containing adhesive, potentially due to the strong interaction between vinylidene fluoride units and oxygen atoms found in MEA.[32] However, in HEMA-containing adhesive, PVDF diluted the SHAM content and the highest adhesive strength was observed for the formulation with 100 wt% SHAM-containing adhesive copolymer.

When the SHAM content in the adhesive copolymer was increased, the recorded S_{adh} values also increased (Fig. 8b and S18†). Average S_{adh} values increased around 2 folds for p(HEMA-*co*-SHAM$_{50}$) and p(MEA-*co*-SHAM$_{50}$) when the feed SHAM content was increased from 10 mol% to 50 mol% during the synthesis of these polymers. These results collectively indicated that the SHAM contributes to strong adhesion. Additionally, both polymers with elevated SHAM content performed equivalently or outperformed a commercial epoxy glue (Fig. 9 and S19†).

The ESI Video S1† captured the tackiness of SHAM-containing adhesive. The precursor solution containing a mixture of p(HEMA-*co*-SHAM$_{10}$) and PVDF (85 : 15 weight ratio) was coated onto the surface of a 100 g, stainless steel weight with a surface area of 258 mm^2. Without drying the adhesive, a glass slide was brought into contact with the adhesive-coated surface (Fig. S20†). The 100 g weight could be lifted almost instantly (<10 seconds of contact) indicating the exceptional tackiness of the adhesive even before the removal of solvents. This simple experiment also demonstrates the adhesive's capability to bond 2 dissimilar surfaces together.

The stability of SHAM-containing adhesive was also explored through various aging analyses. Qualitatively, SHAM-containing adhesive precursor solution exhibited a light yellowish color initially (Fig. S21†). This color did not darken when it was dried on a glass surface or after exposing to air in a lab (temperature ≈21.5 °C, humidity ≈ 20%) for over 5 days. Additionally, ATR-FTIR spectra revealed that peaks associated with SHAM remained unchanged after 5 days (Fig. 10 and S22–S24†). The HEMA-containing sample showed peak broadening and flattening in the C–H stretching region (2800–3063 cm^{-1}, Fig. S23a†) along with a reduction in the intensity of peaks associated with C=O and C=C (Fig. S23b†). Additionally, peaks related to PVDF at 3024 cm^{-1} shifted slightly to 3026 cm^{-1} (Fig. S23c†). However, these peak shifts were relatively minor and the likelihood for polymer hydrolysis,[39] degradation,[40] or oxidation[41] are highly unlikely during the 5-day aging period. No change was observed for the spectra of MEA-containing adhesive.

Finally, lap shear adhesion tests were conducted on SHAM-containing adhesive-bonded joints after they were exposed to open air for 25 days (Fig. 11). p(HEMA-*co*-SHAM$_{10}$) showed no significant change in S_{adh} values over this period. In contrast, p(MEA-*co*-SHAM$_{10}$) exhibited a 20% reduction in S_{adh} values. Similarly, HEMA-containing adhesive exhibited markedly better resistance to incubation in water when compared to

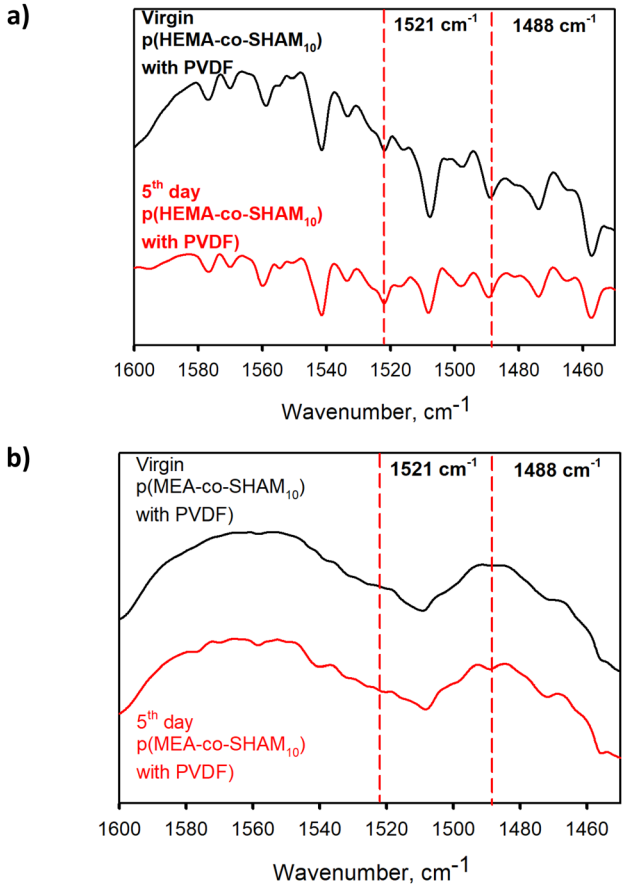

Fig. 10 ATR-FTIR spectra of aging analyzed adhesive showing peaks associated with SHAM (red dashed lines) in the range of 1600–1440 cm^{-1}. The adhesive was prepared with (a) p(HEMA-*co*-$SHAM_{10}$) and (b) p(MEA-*co*-$SHAM_{10}$) with PVDF, containing a copolymer to PVDF weight ratio of 85 : 15.

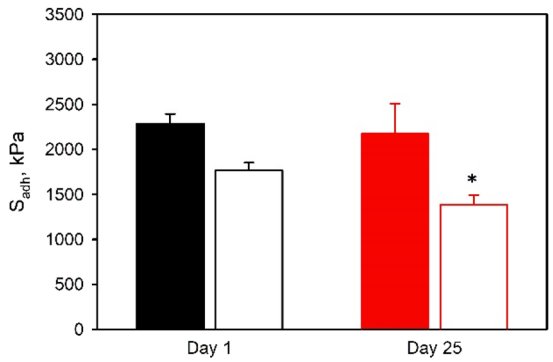

Fig. 11 25-Day aging analysis of adhesively bonded samples exposed to open air (temperature ≈21.5 °C, humidity ≈ 20%). The adhesive was prepared using p(HEMA-*co*-$SHAM_{10}$) (filled bars) and p(MEA-*co*-$SHAM_{10}$) (empty bars) a copolymer to PVDF weight ratio of 85 : 15, with an overlapped area of 64.5 mm^2 and a coating density of 4 mg cm^{-2}. *$p < 0.05$ when compared to the same adhesive formulation tested at Day 1 ($n = 3$).

MEA-containing adhesive (Fig. 12). p(MEA-*co*-$SHAM_{10}$) lost its adhesive property after incubation in water for merely 90 minutes while S_{adh} of p(HEMA-*co*-$SHAM_{10}$) did not change

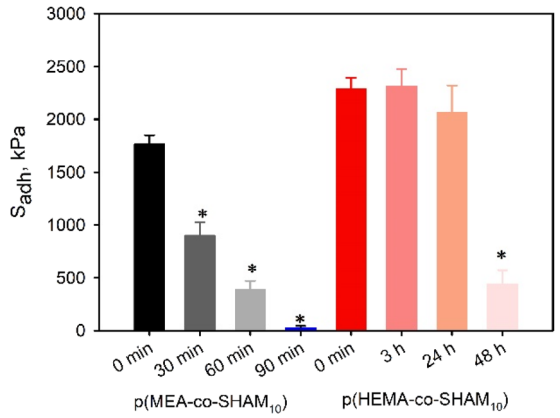

Fig. 12 Effect of duration of incubation in water on S_{adh} for adhesive prepared with a copolymer to PVDF weight ratio of 85 : 15, with an overlapped area of 64.5 mm^2 and a coating density of 4 mg cm^{-2}. *$p < 0.05$ when compared to the samples tested at time = 0 min ($n = 3$).

over 24 hours. The ability for HEMA to form extensive H-bonding likely contributed to improved cohesive property when compared to MEA, which lacks a H-bond donor. However, S_{adh} values of p(HEMA-*co*-$SHAM_{10}$) reduced to only 20% of its initial value after 48 hours of incubation in water. The adhesive formulations reported here are not covalently crosslinked and the relatively hydrophilic nature of the HEMA and MEA likely resulted in the dissolution of the adhesive polymer over time.

Taken together, SHAM demonstrated the ability to function as an adhesive molecule for designing structural adhesives. SHAM-containing adhesives exhibited strong adhesion to multiple types of surfaces, including glass, metallic, and polymeric surfaces. The structural similarity between SHAM and catechol likely enabled SHAM to participate in similar interfacial interactions as those of catechol (*e.g.*, H-bonding, π–π interaction, and cation–π, *etc.*).[42] SHAM is also a known chelator of metal ions,[43] which can potentially facilitate its binding to a metal surface.

The adhesive formulations reported here are not chemically crosslinked. As such, adhesive compositions with increased cohesive interactions resulted in elevated adhesive strength and stability. HEMA consists of a terminal hydroxyl group which contains both a H-bond donor and acceptor. On the other hand, MEA contains a methoxy group and lacks H-bond donors for forming H-bonding. As such, HEMA-containing adhesives demonstrated strong adhesion strength without the need of PVDF, while the MEA-containing adhesive required PVDF to function as a binder to increase its cohesive property. Incorporation of weak H-bonds has been previously utilized to increase the adhesive properties and overall toughness of structural adhesives.[44] For uncrosslinked adhesives, polymers with higher molecular weights result in higher adhesive property because of increased chain entanglement and intermolecular interactions.[45] SHAM-containing polymers were prepared with M_n values of 10^5 Da or higher, which contributed

to the elevated adhesive strength. Although we did not investigate the effect of the molecular weight of PVDF on adhesion, the crystallinity and mechanical properties of PVDF-based materials increase with increasing the molecular weight of PVDF.[46] Increasing the molecular weight of PVDF could potentially be used to further increase the adhesive property of SHAM-containing adhesives.

While the adhesive system reported here demonstrated strong adhesion, it did not demonstrate water resistance. Adhesion strength decreased after soaking the adhesive joint in an aqueous solution over time. The decrease in the measured adhesion strength is likely not due to failure at the interface. Our prior study demonstrated that SHAM exhibited equivalent or better interfacial bonding energy in the presence of water when compared to catechol.[28] The adhesive formulations reported here are not covalently crosslinked and are composed of relatively hydrophilic polymer backbones. The poor water resistance of the adhesive is likely due to the dissolution of the adhesive over time. Future work involving the use of a more hydrophobic backbone or covalent crosslinking could potentially improve the performance of these adhesives in a wet environment.[47,48]

Conclusions

SHAM-containing adhesives were prepared and mixed with PVDF to form a series of new structural adhesives that can bind to multiple types of substrates, including glass, metallic, and polymeric surfaces. Adhesives with elevated SHAM content exhibited adhesive strength as high as 4.8 MPa. SHAM-containing adhesives also demonstrated an S_{adh} value that was 25% higher when compared to that of a catechol-containing adhesive and 27% higher when compared to that of commercial epoxy glue. Additionally, an adhesive composed of a HEMA backbone demonstrated elevated adhesion strength and stability when compared to those prepared with a MEA backbone, due to HEMA's ability to form extensive H-bonding. Adhesive joints prepared using HEMA-containing adhesives were stable for up to 25 days under dry conditions and over 24 hours when submerged in an aqueous solution. SHAM is a promising adhesive molecule for designing new structural adhesives.

Author contributions

The manuscript was written through contributions of all authors. All authors have given approval to the final version of the manuscript.

Data availability

The data supporting this article have been included as part of the ESI.†

Conflicts of interest

There are no conflicts to declare.

Acknowledgements

The authors acknowledge Dr Andrew Gross (Managing Director, Microfabrication Facility, Michigan Technological University) and Machine Shop facility (Manufacturing and Mechanical Engineering Technology, Michigan Technological University). This project was funded by the Office of Naval Research under award numbers N00014-20-1-2230 and N00014-21-1-2877, the National Science Foundation under award number CMMI 2119019 and the National Institutes of Health under award number R15GM135875.

References

1 X. He, W. Wang, S. Yang, F. Zhang, Z. Gu, B. Dai, T. Xu, Y. Y. S. Huang and X. Zhang, *Appl. Phys. Rev.*, 2023, **10**, 011305.
2 S. Nam and D. Mooney, *Chem. Rev.*, 2021, **121**, 11336–11384.
3 A. Sezinando, *Rev. Port. Estomatol. Med. Dent. Cir. Maxilofac.*, 2014, **55**, 194–206.
4 F. Versino, F. Ortega, Y. Monroy, S. Rivero, O. V. López and M. A. García, *Foods*, 2023, **12**, 1057.
5 F. Cavezza, M. Boehm, H. Terryn and T. Hauffman, *Metals*, 2020, **10**, 730.
6 M. Almeida, R. L. Reis and T. H. Silva, *Mater. Sci. Eng., C*, 2020, **108**, 110467.
7 W. Zhang, R. Wang, Z. Sun, X. Zhu, Q. Zhao, T. Zhang, A. Cholewinski, F. Yang, B. Zhao, R. Pinnaratip, P. K. Forooshani and B. P. Lee, *Chem. Soc. Rev.*, 2020, **49**, 433–464.
8 K. Gan, C. Liang, X. Bi, J. Wu, Z. Ye, W. Wu and B. Hu, *Front. Bioeng. Biotechnol.*, 2022, **10**, 870445.
9 Q. Guo, J. Chen, J. Wang, H. Zeng and J. Yu, *Nanoscale*, 2020, **12**, 1307–1324.
10 P. K. Forooshani and B. P. Lee, *J. Polym. Sci., Part A: Polym. Chem.*, 2017, **55**, 9–33.
11 Y. Ma, B. Zhang, I. Frenkel, Z. Zhang, X. Pei, F. Zhou and X. He, in *Progress in Adhesion and Adhesives*, 2021, pp. 739–759.
12 J. H. Waite, *Int. J. Adhes. Adhes.*, 1987, **7**, 9–14.
13 B. P. Lee, P. B. Messersmith, J. N. Israelachvili and J. H. Waite, *Annu. Rev. Mater. Res.*, 2011, **41**, 99–132.
14 Q. Lu, E. Danner, J. H. Waite, J. N. Israelachvili, H. Zeng and D. S. Hwang, *J. R. Soc., Interface*, 2013, **10**, 20120759.
15 A. A. Putnam and J. J. Wilker, *Soft Matter*, 2021, **17**, 1999–2009.
16 H. Lee, N. F. Scherer and P. B. Messersmith, *Proc. Natl. Acad. Sci. U. S. A.*, 2006, **103**, 12999–13003.

17 A. R. Narkar, B. Barker, M. Clisch, J. Jiang and B. P. Lee, *Chem. Mater.*, 2016, **28**, 5432–5439.
18 M. S. A. Bhuiyan, J. D. Roland, B. Liu, M. Reaume, Z. Zhang, J. D. Kelley and B. P. Lee, *J. Am. Chem. Soc.*, 2020, **142**, 4631–4638.
19 K. Pillai, B. Costello, C. Oresajo and J. Ceccoli, *Us. Pat.*, 20060165641A1, 2006.
20 T. Urbański, *Nature*, 1950, **166**, 267–268.
21 S. S. Hassan, R. M. El-Bahnasawy and N. M. Rizk, *Anal. Chim. Acta*, 1997, **351**, 91–96.
22 V. Puca, G. Turacchio, B. Marinacci, C. T. Supuran, C. Capasso, P. Di Giovanni, I. D'Agostino, S. Carradori and R. Grande, *Int. J. Mol. Sci.*, 2023, **24**, 4455.
23 Y. Ji, X. Li, K. Jin, Z. Fan, K. Hou, P. Du, B. Xu and Z. Cai, *Fibers Polym.*, 2024, **25**, 1–33.
24 D. Grigorieva, I. Gorudko, V. Reut, A. Simakin, V. Kostevich, N. Gorbunov, O. Panasenko and A. Sokolovc, *J. Appl. Spectrosc.*, 2024, **91**, 1–10.
25 B. Dong, P. Wang, Z. Li and Y. Tan, *Arabian J. Chem.*, 2023, **16**, 105048.
26 B. Suslavich, R. LaDouceur, A. Mamudu and C. Young, *Miner. Miner. Mater.*, 2024, **3**, 1.
27 K. Cui, S. Jin and N. Duan, *Powder Technol.*, 2023, **427**, 118705.
28 K. Wang, L. Patra, B. Liu, Z. Zhang, R. Pandey and B. P. Lee, *Chem. Mater.*, 2023, **35**, 5322–5330.
29 Y. Bu and A. Pandit, *Bioact. Mater.*, 2022, **13**, 105–118.
30 C. Ouyang, H. Yu, L. Wang, Z. Ni, X. Liu, D. Shen, J. Yang, K. Shi and H. Wang, *Adv. Colloid Interface Sci.*, 2023, **319**, 102982.
31 J.-E. Lee, Y.-E. Shin, G.-H. Lee, J. Kim, H. Ko and H. G. Chae, *Composites, Part B*, 2021, **223**, 109098.
32 T. V. Terziyan and A. P. Safronov, *J. Mol. Liq.*, 2019, **275**, 378–383.
33 A. Akthakul, R. F. Salinaro and A. M. Mayes, *Macromolecules*, 2004, **37**, 7663–7668.
34 L. Zhao, Z. Sun, H. Zhang, Y. Li, Y. Mo, F. Yu and Y. Chen, *RSC Adv.*, 2020, **10**, 29362–29372.
35 Y. Wu, X. Du, R. Gao, J. Li, W. Li, H. Yu, Z. Jiang, Z. Wang and H. Tai, *Nanoscale Res. Lett.*, 2019, **14**, 1–9.
36 X. Chen, X. Han and Q. D. Shen, *Adv. Electron. Mater.*, 2017, **3**, 1600460.
37 M. S. A. Bhuiyan, J. Manuel, F. Razaviamri and B. P. Lee, *ACS Appl. Polym. Mater.*, 2023, **5**, 3949–3957.
38 S. Lanceros-Méndez, J. F. Mano, A. M. Costa and V. H. Schmidt, *J. Macromol. Sci. Phys. B*, 2001, **40**, 517–527.
39 H. S. Mansur, C. M. Sadahira, A. N. Souza and A. A. Mansur, *Mater. Sci. Eng., C*, 2008, **28**, 539–548.
40 B. N. Jang and C. A. Wilkie, *Polym. Degrad. Stab.*, 2004, **86**, 419–430.
41 H. Y. Tan, E. Widjaja, F. Boey and S. C. J. Loo, *J. Biomed. Mater. Res., Part B*, 2009, **91**, 433–440.
42 J. Kim, C. Lee and J. H. Ryu, *Appl. Sci.*, 2020, **11**, 21.
43 S. N. Kane, A. Gupta, S. M. Ali and P. V. Khadikar, *Hyperfine Interact.*, 1987, **35**, 927–930.
44 M. G. Mazzotta, A. A. Putnam, M. A. North and J. J. Wilker, *J. Am. Chem. Soc.*, 2020, **142**, 4762–4768.
45 C. L. Jenkins, H. J. Meredith and J. J. Wilker, *ACS Appl. Mater. Interfaces*, 2013, **5**, 5091–5096.
46 B. Zaarour, L. Zhu and X. Jin, *Soft Mater.*, 2019, **17**, 181–189.
47 Q. Du, B. Hu, Q. Shen, S. Su, S. Wang and G. Song, *Chem. Eng. J.*, 2024, **482**, 148828.
48 H. J. Meredith, C. L. Jenkins and J. J. Wilker, *Adv. Funct. Mater.*, 2014, **24**, 3259–3267.